INFECTION AND IMMUNITY, Oct. 2006, p. 5465–5476 Vol. 74, No. 10
0019-9567/06/$08.00+0 doi:10.1128/IAI.00737-06

Genome-Wide Expression Analysis of *Burkholderia pseudomallei* Infection in a Hamster Model of Acute Melioidosis

Apichai Tuanyok,[1] Marina Tom,[1] John Dunbar,[2] and Donald E. Woods[1]*

Department of Microbiology and Infectious Diseases, Faculty of Medicine, University of Calgary Health Sciences Centre, 3330 Hospital Drive, NW, Calgary, Alberta, Canada T2N 4N1,[1] and Biosciences Division, Los Alamos National Laboratory, Los Alamos, New Mexico 87545[2]

Received 8 May 2006/Returned for modification 20 June 2006/Accepted 28 July 2006

Burkholderia pseudomallei **is the causative agent of melioidosis and represents a potential bioterrorism threat. In the current studies we have examined gene expression in *B. pseudomallei* in an animal model of acute melioidosis using whole-genome microarrays. Gene expression profiles were generated by comparing transcriptional levels of *B. pseudomallei*-expressed genes in infected hamster organs including liver, lung, and spleen following intraperitoneal and intranasal routes of infection to those from bacteria grown in vitro. Differentially expressed genes were similar in infected livers irrespective of the route of infection. Reduced expression of a number of housekeeping genes suggested a lower bacterial growth rate during infection. Energy production during growth in vivo involved specific biochemical pathways such as isomerization of 3-phosphoglycerate, catabolism of D-glucosamine and inositol, and biosynthesis of particular amino acids. In addition, the induction of genes known to be involved in oxidative phosphorylation including ubiquinol oxidase, ferredoxin oxidoreductase, and formate dehydrogenase enzymes suggested the use of alternative pathways for energy production, while the expression of genes coding for ATP-synthase and NADH-dehydrogenase enzymes was reduced. Our studies have identified differentially expressed genes which include potential virulence genes such as those for a putative phospholipase C and a putative two-component regulatory system, and they have also provided a better understanding of bacterial metabolism in response to the host environment during acute melioidosis.**

Melioidosis is a major tropical disease prevalent in Southeast Asia and northern Australia (6, 8). This disease was first described in 1912 by Whitmore and Krishnaswami in Rangoon, Myanmar (37). The disease is fatal and is caused by a soil bacterium, *Burkholderia pseudomallei*. Infection can occur from soil or water contamination of skin abrasions or inhalation of *B. pseudomallei* from natural sources. Sporadic cases of melioidosis have been reported worldwide (29). These include travelers who have returned from areas of endemicity, especially during the tsunami disaster in Southeast Asian countries in December 2004 (1).

B. pseudomallei is a common cause of human pneumonia and septicemias in areas of endemicity (4). The disease may become dormant, and the infected person may relapse after months, years, or decades (26). In northeastern Thailand, melioidosis accounts for as much as 20% of community-acquired septicemias and causes death in 40% of treated patients (36). At present there are no effective vaccines against *B. pseudomallei* infection.

Several in vitro studies have demonstrated a better understanding of pathogenesis and virulence of *B. pseudomallei* in tissue culture models. The bacterium can invade both phagocytic and nonphagocytic cells followed by intracellular multiplication and intercellular spread (15, 16). However, the mechanisms for bacterial survival in host tissues are not fully understood. In addition, a variety of eukaryotic host models for *B. pseudomallei* infection have been used to study bacterial virulence and to identify virulence determinants. Hosts studied include *Caenorhabditis elegans* (12, 27) and higher animals (19). The use of animal infection models in combination with bacterial genetics and immunological and antigen purification techniques can teach us much about the pathogenesis of diseases due to microorganisms (38). The hamster model of acute melioidosis was first used to study experimental chemotherapy of melioidosis by Miller and colleagues in 1948 (23), and the model has been used extensively to assess the relative virulence of *B. pseudomallei* (3, 34). Hamsters are exquisitely sensitive to *B. pseudomallei* infection and do not display individual variation in susceptibility to *B. pseudomallei* (10).

In the present studies, we used microarray techniques to compare differential gene expression in *B. pseudomallei* during infection of Syrian hamsters to gene expression in *B. pseudomallei* grown in vitro. Our studies have identified potential virulence determinant genes as well as providing interesting information regarding the bacterial metabolic response to the host environment.

MATERIALS AND METHODS

Bacterial strains, plasmids, and growth conditions. Bacterial strains and plasmids used in this study are listed in Table 1. To isolate bacterial RNA from the broth culture, *B. pseudomallei* 1026b was grown in Luria-Bertani (LB) broth at 37°C with shaking at 250 rpm. The bacterial cells were harvested when the cell growth reached an optical density at 600 nm of 0.9, equivalent to mid-exponential-phase growth.

Animal studies and routes of infection. Two different routes of infection were used in this study, intraperitoneal (i.p.) and intranasal (i.n.). Syrian hamsters (female, 6 to 8 weeks of age) were used throughout the studies.

(i) Intraperitoneal route of infection. Five hamsters were injected with a 100-μl suspension of organisms grown in LB. Serial dilutions were made in

* Corresponding author. Mailing address: Department of Microbiology and Infectious Diseases, Faculty of Medicine, University of Calgary Health Sciences Centre, 3330 Hospital Drive, NW, Calgary, Alberta, Canada T2N 4N1. Phone: (403) 220-2564. Fax: (403) 210-8504. E-mail: woods@ucalgary.ca.

TABLE 1. Bacterial strains and plasmids used in this study

Bacterial strain or plasmid	Description	Reference or source
Strains		
B. pseudomallei		
1026b	Clinical isolate; Gm^r Sm^r Px^r Tp^s	11
DD503	1026b derivative; Δ(*amrR-oprA*) *rpsL* (Sm^r) AG^s Tc^s	24
ATL0378	DD503 derivative; ΔBPSL0378 Gm^r	This study
ATL1876	DD503 derivative; ΔBPSL1876 Gm^r	This study
ATL2025	DD503 derivative; ΔBPSL2025 Gm^r	This study
ATL2515	DD503 derivative; ΔBPSL2515 Gm^r	This study
ATL3050	DD503 derivative; ΔBPSL3050 Gm^r	This study
ATL3320	DD503 derivative; ΔBPSL3320 Gm^r	This study
ATS0067	DD503 derivative; ΔBPSS0067 Gm^r	This study
ATS0464	DD503 derivative; ΔBPSS0464 Gm^r	This study
ATS1388	DD503 derivative; ΔBPSS1388 Gm^r	This study
ATS1489	DD503 derivative; ΔBPSS1489 Gm^r	This study
ATS1530	DD503 derivative; ΔBPSS1530 Gm^r	This study
ATCPL2025	ATL2025 carrying pCPL2025; Gm^r Tmp^r	This study
ATCPS0067	ATS0067 carrying pCPS0067; Gm^r Tmp^r	This study
E. coli		
TOP10	General cloning and blue-white screening.	Invitrogen
SM10λ*pir*	*E. coli* cloning strain	30
S17-1	*E. coli* cloning strain	30
Plasmids		
pCR2.1-TOPO	3.9-kb TA cloning vector; pMB1 oriR Ap^r Km^r	Invitrogen
pGSV3-*lux*	Mobilizable suicide vector containing *lux* operon from pSC26; oriT Gm^r	25
pUCP28T	Shuttle vectors derived from pUC18/19; Tmp^r	35
PCPL2025	(BamHI-XbaI)-pUCP28T::full BPSL2025; Tmp^r	This study
PCPS0067	(BamHI-XbaI)-pUCP28T::full BPSS0067; Tmp^r	This study

phosphate-buffered saline to obtain an infective dose 10 times higher than the known 50% lethal dose (LD_{50}) of *B. pseudomallei* 1026b (11). Serial dilution and plate counts were used to confirm the dose. All hamsters were severely ill at 40 h after the inoculation. At this time, all hamsters were euthanized, and the infected organs were immediately collected. The infected lungs, spleens, and livers were preserved in RNA*later* solution (Ambion) at −70°C until required.

(ii) Intranasal route of infection. Five hamsters were infected with *B. pseudomallei* 1026b via the intranasal route. After the hamsters were anesthetized with 8 mg of ketamine, a 20-μl suspension of organisms grown in LB was intranasally inoculated into one nostril of each hamster. The infective dose confirmed by serial dilution and plate count was approximately 10^6 CFU. All hamsters were ill at 40 h after the inoculation. The hamsters were euthanized, and the infected organs including the livers, lungs, and spleens were collected as described for the intraperitoneal inoculation experiments and preserved in RNA*later* solution (Ambion) at −70°C until required.

RNA isolation. (i) Bacterial total RNA from broth culture. Bacterial cells were harvested from 20 ml broth culture in LB at an optical density at 600 nm of 0.9. Prior to harvest of the cells, 1% (vol/vol) of RNA*later* was added to the culture and maintained at 4°C. The bacterial cells were harvested by centrifugation at 8,000 × *g* at 4°C for 5 min. The cell pellets were treated with 1 ml of Trizol solution (Invitrogen), mixed well, and maintained at room temperature for 5 min. Two hundred microliters of chloroform was added and mixed for 20 seconds. The mixture was maintained at room temperature for 10 min. The tube was centrifuged at 10,000 × *g* at 4°C for 15 min, and the aqueous phase was transferred to a fresh tube containing 1 ml of isopropanol, mixed well, and maintained at room temperature for 10 min. The tube was centrifuged at 10,000 × *g* at 4°C for 15 min. At this step, the total RNA pellet was precipitated. The supernatant was carefully discarded, and the pellet was washed with 1 ml of 75% ethanol by centrifugation at 10,000 × *g* at 4°C for 5 min. The RNA pellet was dried at room temperature. The pellet was resuspended in 30 μl of the RNase-free distilled water and treated with DNase I (DNA-*free*; Ambion Inc.). RNA concentration was quantified by spectrophotometry, and samples were electrophoresed in a formaldehyde agarose gel to assess the quality of RNA.

(ii) Bacterial total RNA from infected tissues. The infected hamsters' organs preserved in RNA*later* were thawed at room temperature. RNA isolation from each organ was performed independently using the same protocol. Briefly, the RNA*later* solution was removed from the container and then 2, 3, and 5 ml of Trizol were added to the samples of spleen, lung, and liver, respectively. Samples were homogenized with a Brinkman Polytron homogenizer, and the homogenized samples were maintained at room temperature for 5 min. The samples were divided, and 1 ml each was placed into microcentrifuge tubes. To each tube was added 200 μl of chloroform, and tubes were maintained at room temperature for 10 min. The tubes were centrifuged at 10,000 × *g* at 4°C for 15 min. After centrifugation, the aqueous phase was transferred to a fresh tube containing 1 ml of isopropanol, mixed well, and maintained at room temperature for 10 min. The following steps were preceded by the same procedure as that for the bacterial total RNA isolation described above, but the product from this step was a mixture of total RNA from eukaryotic cells and bacterial cells. After removal of contaminating DNA with DNase I, the total bacterial RNA was purified from the mixture using Microb*Enrich* (Ambion) per the manufacturer's instructions. Briefly, 100 μg (volume no larger than 30 μl) of the mixed RNA was combined with 300 μl of binding buffer and gently mixed. Forty microliters of the Capture Oligo Mix (containing oligonucleotides specific for eukaryotic RNA) was added to the mixture and then heated at 70°C for 10 min. This heat denaturation helped to facilitate maximal hybridization of the capture oligonucleotide to the mammalian RNA. The mixture was then incubated at 37°C for 1 h. In the meantime, the Oligo Magbeads (containing sequences for specific binding to the Capture Oligo Mix and conjugated with magnetic beads) was prepared by being washed with nuclease-free water and resuspended in the binding buffer using 500 μl of Oligo Magbeads per 100 μg of input RNA. After incubation, the RNA mixture and the Oligo Magbeads were combined and further incubated at 37°C for 10 min. The Oligo Magbeads containing the eukaryotic RNA were captured to one side of the tube's inner wall using the magnetic stand. The supernatant containing the total bacterial RNA was transferred to a fresh tube, further precipitated in ethanol, and centrifuged. The total bacterial RNA was resuspended in nuclease-free water. The total bacterial RNA purified from this technique yielded approximately 10% by weight of the input RNA.

(iii) Bacterial mRNA purification. Bacterial mRNA purification was used to purify the bacterial mRNA from the total bacterial RNA from both sources described above using MICROB*Express* (Ambion Inc.) per the manufacturer's instructions. Briefly, 2 to 10 μg (volume no larger than 15 μl) of the bacterial total RNA was mixed with 200 μl of binding buffer. Four microliters of Capture Oligo mix was added to the mixture and incubated at 70°C for 10 min. This heat denaturation helped to facilitate maximal hybridization of the rRNA to the capture oligonucleotides. The tube was incubated further at 37°C for 15 min. In the meantime, 50 μl of Oligo Magbeads (containing sequences for specific binding to the capture oligonucleotides and conjugated with magnetic beads) was prepared by being washed with nuclease-free water, resuspended with the binding buffer, and incubated at 37°C until required. Fifty microliters of the prepared Oligo Magbeads was added to the mixture and incubated further at 37°C for 15 min. This step allowed the hybridization of Oligo Magbeads and allowed the capture oligonucleotide with rRNA to be formed. The Oligo Magbeads containing the rRNA were captured to one side of the tube's inner wall using the magnetic stand. The supernatant containing the purified bacterial mRNA was transferred to a fresh tube, further precipitated in ethanol, and centrifuged. The mRNA was resuspended in nuclease-free water. The mRNA purified from this technique yielded approximately 10% and 80% by weight of the input total RNA previously isolated from LB culture and from the Microb*Enrich* purified total RNA of the infected organs, respectively.

Examination of bacterial RNA by a quantitative RT-PCR. All bacterial total RNA and mRNA obtained after purification were analyzed by reverse transcription-PCR (RT-PCR) to quantify the presence of the 16S and 23S rRNA. One-step RT-PCR was used as previously described (33). PCR primers for the 16S and 23S rRNA are shown in Table 2.

Microarray analysis. Microarray analyses were performed as previously described (33) with minor modifications. Briefly, equal amounts of 3 to 5 μg of bacterial mRNA obtained from both sources (LB culture and infected organ) were annealed with 10 μg of the random hexamer $pd(N)_6$ (Amersham Bio-

TABLE 2. PCR primers used in this study

Gene	Primer name	Nucleotide sequence, 5′ to 3′	Purpose
BPSL0378	L0378-for	CAAAGGCTCCCGATGAGCGA	Internal PCR
	L0378-rev	AAATGTCGGCATCGAGCGCC	Internal PCR
	Up-L0378-for	GAAATTCGTGTCGAGCTGCG	Merodiploid confirmation
BPSL1876	L1876-for	GGTCGGCGTCTACCGGAT	Internal PCR
	L1876-rev	TCGAGGAACGTGAACGCGGG	Internal PCR
	Up-L1876-for	CCCAACGGAGTCCGCTCGT	Merodiploid confirmation
BPSL2025	L2025-for	ACCGCGACCTGAAGCGGCT	Internal PCR
	L2025-rev	GATCGACACGACCCGCCC	Internal PCR
	Up-L2025-for	TCGCGTTCCTGACGCTGCC	Merodiploid confirmation
	CPL2025-for	CCATAAGCGGAACGCCGCAG	Complementation of ΔBPSL2025
	CPL2025-rev	TCGATACGTCGCCCATGCCC	Complementation of ΔBPSL2025
BPSL2515	L2515-for	ATCAGGGCGAGGTTGAGGTT	Internal PCR
	L2515-rev	ATGCGATGTCGGTGATGTG	Internal PCR
	Up-L2515-for	CGAACAGGTGCTCGCGTG	Merodiploid confirmation
BPSL3050	L3050-for	CCAACGAGGGCTACAACCGC	Internal PCR
	L3050-rev	GCACGCTCGCCGACGTGA	Internal PCR
	Up-L3050-for	AATTCGGCAGGATCAGCG	Merodiploid confirmation
BPSL3320	L3320-for	GCCCTCGACGGGCAATTCGT	Internal PCR
	L3320-rev	TTGCGACCATGCGACGCTGC	Internal PCR
	Up-L3320-for	GTCGACTTCGGCAACCAGCG	Merodiploid confirmation
BPSS0067	S0067-for	GATACCCGCCTTCGTCATCT	Internal PCR
	S0067-rev	CAGCGTGCCGAAGTAGTTG	Internal PCR
	Up-S0067-for	GATACCCGCCTTCGTCATCT	Merodiploid confirmation
	CPS0067-for	CTCGATGTGCAACGCCGCC	Complementation of ΔBPSS0067
	CPS0067-rev	CCATTGTCGTGCGCGTCAGG	Complementation of ΔBPSS0067
BPSS0464	S0464-for	GGTCAGGCTTCTCGCTGAAG	Internal PCR
	S0464-rev	TGATGAAGAGCGTCGCGAGC	Internal PCR
	Up-S0464-for	GGCTATCCGATGGCGTACTA	Merodiploid confirmation
BPSS1388	S1388-for	GCGAATCTCGCGAAAGCGGA	Internal PCR
	S1388-rev	CCAGTCTCTTGGCGACCTTC	Internal PCR
	Up-S1388-for	TGTTCCGGCAACTCGAAACG	Merodiploid confirmation
BPSS1489	S1489-for	GCGACGGCAACCGATTCGCT	Internal PCR
	S1489-rev	ACTGAATGCCGAGCAGCGCG	Internal PCR
	Up- S1489-for	GCGACGGCAACCGATTCGCT	Merodiploid confirmation
BPSS1530	S1530-for	AAGGAACTGAAGGCTCGGGC	Internal PCR
	S1530-rev	TCCATTTCGGCTCGATGCCG	Internal PCR
	Up-S1530-for	AAGAACCAGATCGACGGCGC	Merodiploid confirmation
luxC	*luxC*-rev	ACGAATGTATGTCCTGCGTCTTGAG	pGSV3-*lux* fusion and merodiploid confirmation
16S rRNA	16S rRNA-for	TGGCTAATACCCGGAGTGGA	RT-PCR
	16S rRNA-rev	CGGTTTGTCACCGGCAGTCT	RT-PCR
23S rRNA	23S rRNA-for	GCCAGCTAAGGTCCCCAAAT	RT-PCR
	23S rRNA-rev	TGCAGGTCGGAACTTACCCG	RT-PCR

science) by incubation at 70°C for 10 min and maintained on ice. The cDNA was generated in a reverse transcription reaction using 100 U of StrataScript reverse transcriptase, 2 μl of 10× StrataScript reaction buffer, 1 μl of 20× deoxynucleoside triphosphate mix with an amino-allyl-dUTP, 1.5 μl of 0.1 M dithiothreitol, and 0.5 μl of 40 U μl^{-1} of RNase block (Stratagene Inc.). The reaction mixture was incubated at 48°C for 1 h 30 min. The amino-allyl cDNAs from both samples were labeled differently with 5 μl of Cy3 or Cy5 (Cy^3-, Cy^5-monofunctional dyes; Amersham Bioscience) at room temperature for 30 min in the dark. The uncoupled dye was removed from the fluorescent dye-labeled cDNA by using a microspin cup and DNA binding solution (Stratagene Inc.), and the volume was reduced to approximately 3 μl by vacuum centrifugation. Each Cy3- and Cy5-labeled cDNA was diluted with hybridization solution containing 4× SSC (1× SSC is 0.15 M NaCl plus 0.015 M sodium citrate) and 0.1% sodium dodecyl sulfate. Both hybridization solutions were combined and mixed carefully by pipetting and then heated at 95°C for 3 min. Volumes of the hybridization were 50 μl. The hybridization solution was left to cool at room temperature and mixed thoroughly by centrifugation. The hybridization solution was applied onto the microarray and covered with a plastic coverslip. The slide was incubated at 50°C in a slide hybridization chamber (Boekel Scientific) for 18 h. Following incubation, the slide was washed with four

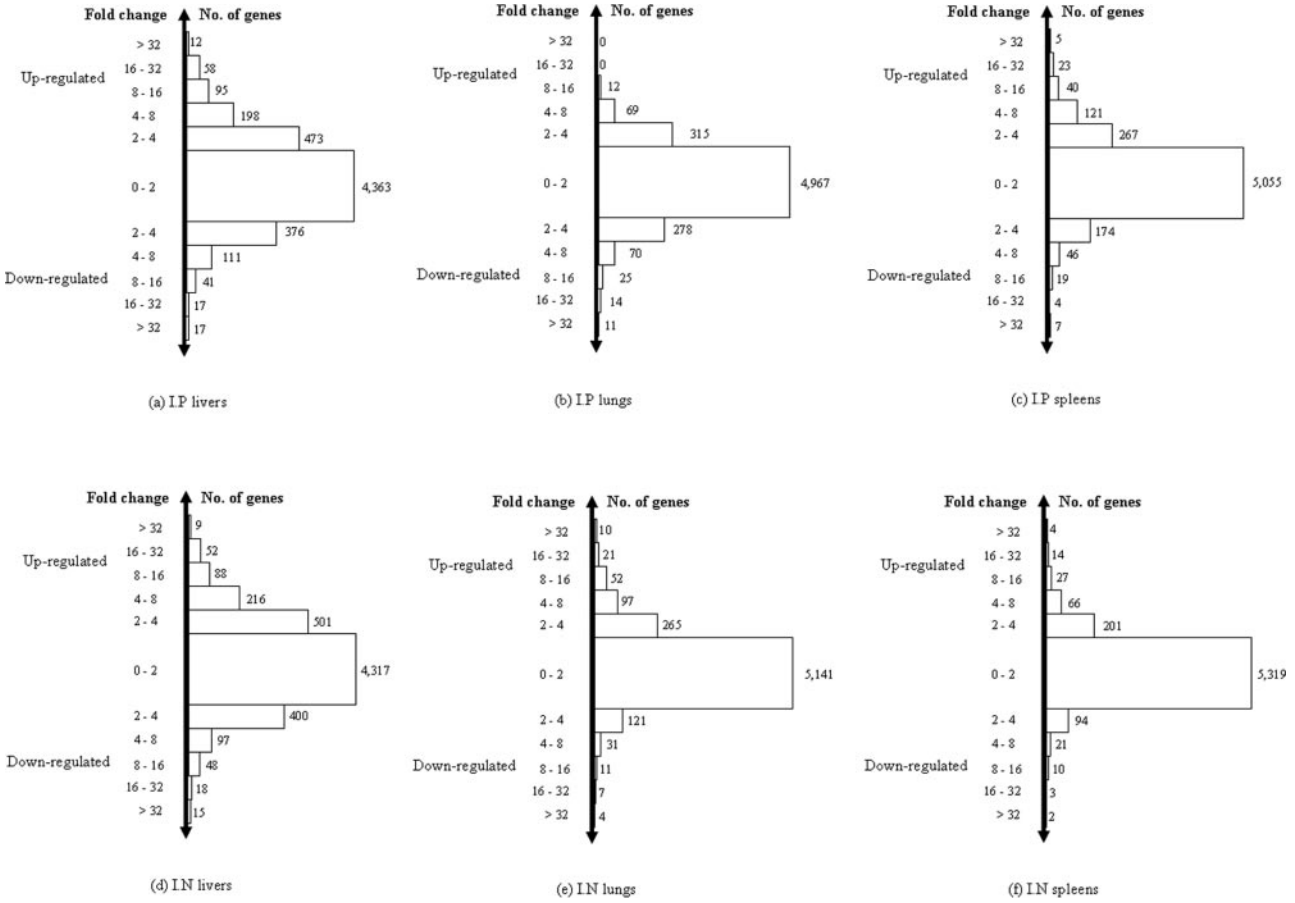

FIG. 1. Genes grouped according to expression levels (changes [*n*-fold]) from six organ infection models (i.p. infected liver, i.p. infected lung, i.p. infected spleen, i.n. infected liver, i.n. infected lung, and i.n. infected spleen). The highest numbers of up- or down-regulated genes were from infected livers (a and d) for both routes of infection.

solutions: solution 1, 4× SSC, 0.2% (wt/vol) sodium dodecyl sulfate for 5 min at 50°C, twice; solution 2, 0.2× SSC for 1 min; and solution 3, 0.1× SSC for 1 min each at room temperature. The slide was spin dried in a centrifuge at 550 rpm for 5 min and scanned immediately. Scanning was performed with a Virtek ChipReader (Virtek Biotech, Canada). The fluorescence signals from both dyes were quantified using QuantArray microarray analysis software (Packard Bioscience). Normalization and data analysis were performed with GeneTraffic software (Iobion Informatics). Data obtained from at least 24 hybridizations of two independent RNA preparations of each type of infected organ including flip-dye replications were used in each analysis. Normalization of data was performed on each hybridization using LOWESS (Locally Weighted Scatter Plot Smoother), a curve-fitting algorithm.

Calculation and statistical analysis. To select significantly expressed genes from the whole-genome microarray data, basic calculation and statistics including differences (*n*-fold), mean $\log_2$ ratio, standard deviation (SD), coefficient of variance (COV), and Student's *t* test were used in the analysis. Hierarchical clustering and K-mean clustering analyses were performed using TIGR-MeV software (www.tigr.org).

Microarray data repository. Raw microarray data from this study are available at ftp://136.159.173.80/. Further information is available upon request.

Construction of insertion mutants. Insertion mutations were constructed in 11 up-regulated genes including BPSL0378 (MarR family regulatory protein), BPSL1876 (putative phospholipase), BPSL2025 (putative two-component regulatory system), BPSL2515 (*rpsA*; 30S ribosomal protein S1), BPSL3320 (*fliD*; flagellar hook-associated protein), BPSL3050 (*trpE*; anthranilate synthase component I), BPSS0067 (putative phospholipase C precursor), BPSS0464 (*potI*, putrescine transport system permease protein), BPSS1388 (putative membrane protein), BPSS1489 (putative exported protein), and BPSS1530 (*bprA*, putative H-NS-like regulatory protein).

A previously described *lux*-based suicide vector, pGSV3-*lux*, was used in this study (25). Briefly, an internal region of approximately 300 to 600 bp of those 11 selected genes was amplified by PCR. The PCR products were cloned with pCR2.1-TOPO (Invitrogen). The recombinant plasmid was digested with EcoRI, and a small fragment (the insert) was purified and ligated into EcoRI-digested, calf intestinal alkaline phosphatase-treated pGSV3-*lux*. The recombinant plasmids were transformed into *Escherichia coli* SM10λ*pir* or S17-1 (30). The transformed *E. coli* containing the recombinant pGSV3-*lux* plasmid was conjugated with *B. pseudomallei* DD503 (24), and transconjugants were selected on LB-gentamicin-polymyxin B agar. The transconjugants were screened for *lux*-mediated light production by assaying 100 μl of overnight broth cultures of individual colonies. Cultures which displayed light production were then tested for insertion of pGSV3-*lux* into the target gene using PCR. *B. pseudomallei* strains ATL0378, ATL1876, ATL2025, ATL2515, ATL3320, ATL3050, ATS0067, ATS0464, ATS1388, ATS1489, and ATS1530 were insertion mutant derivatives based on genes BPSL0378, BPSL1876, BPSL2025, BPSL2515, BPSL3320, BPSL3050, BPSS0067, BPSS0464, BPSS1388, BPSS1489, and BPSS1530, respectively.

Virulence assessment of mutant strains. The animal model of acute melioidosis has been previously described (10). Syrian hamsters (females, 6 to 8 weeks old) were intraperitoneally challenged with a 100-μl suspension of a diluted mid-exponential-phase culture of the 11 *B. pseudomallei* mutant strains containing 100 CFU (10 times higher than LD_{50} of DD503) of bacteria. The number of dead animals in each group (five per group) was determined after 48 h. LD_{50} evaluation was performed only for the mutant strains which demonstrated less virulence at this infective dose. The LD_{50} evaluation was performed with a number of serial dilutions corresponding to 10^1 to 10^5 CFU of the mutant strains, and the LD_{50} values were calculated using the Reed and Muench method (28). All animals used in these studies were cared for and used humanely according to the

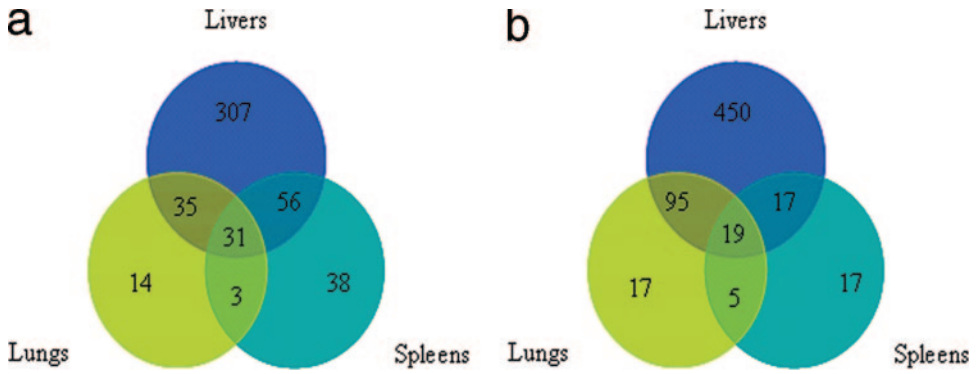

FIG. 2. Venn diagrams showing numbers of common genes differentially expressed in each organ and associated with routes of infection, intraperitoneal (a) and intranasal (b). These genes were selected using the COV applied to an individual infected organ (total of two organs).

Guide to the Care and Use of Experimental Animals published by the Canadian Council on Animal Care.

Complementation of ΔBPSL2025 and ΔBPSS0067 mutants. DNA fragments of full BPSL2025 or BPSS0067 genes including the upstream promoter region were amplified from *B. pseudomallei* 1026b genomic DNA by PCR using the primers listed in Table 2. Both PCR products were cloned as a BamHI-XbaI fragment into pUCP28T (35) to generate recombinant plasmids, pCPL2025 and pCPS0067. *E. coli* SM10λ*pir* containing recombinant plasmid pCPL2025 or pCPS0067 was conjugated to *B. pseudomallei* ATL2025 or ATS0067, respectively, and Tmp^r colonies were screened by plasmid DNA isolation to confirm the presence of pCPL2025 and pCPS0067 in the mutant strains.

RESULTS

Comparative gene expression profiles of in vivo- and in vitro-grown *B. pseudomallei*. Syrian hamsters were infected with *B. pseudomallei* 1026b intraperitoneally and intranasally. Gene expression profiles were obtained from a comparison of transcriptional levels of expressed genes observed in each infected organ including liver, lung, and spleen with those from bacterial growth at mid-exponential phase in LB medium. To select differentially expressed genes, we initially grouped genes according to their expression levels as seen in Fig. 1. We then applied a COV value of ≤0.25 to the group of genes which had low expression levels, i.e., levels between twofold and less-than-fourfold different ($1 \leq \log_2$ ratio < 2 or $-2 < \log_2$ ratio ≤ -1), and a COV value of ≤0.5 to the groups containing high expression levels, i.e., levels at least fourfold different ($2 \leq \log_2$ ratio ≤ -2). Subsequently, gene lists from those two groups were combined and defined as differentially expressed genes. The SD of the selected genes did not exceed 25% and 50% of the mean $\log_2$ ratio from those low- and high-relative-expression groups, respectively. This ensured that the selected genes were chosen from consistently expressed genes, and the minimum difference defined as significant was 1.68-fold ($\log_2$ ratio = 0.75). Thus, 429, 83, and 128 genes were differentially expressed in liver, lung, and spleen, respectively, in i.p. infected animals. In i.n. infected animals, 581, 136, and 58 genes were differentially expressed from liver, lung, and spleen, respectively. A total of six organ infection models (i.p. infected liver, i.p. infected lung, i.p. infected spleen, i.n. infected liver, i.n. infected lung, and i.n. infected spleen) were generated from this study; gene lists and details are shown in Tables 1 to 6 posted at ftp://136.159.173.80/. We noted that the highest numbers of differentially expressed genes in animals infected intraperitoneally or intranasally were seen in infected liver.

We searched for common genes among those six organ infection models using two different criteria: (i) common genes and routes of infection and (ii) common genes and types of infected organs.

(i) Common genes and routes of infection. Venn diagrams in Fig. 2 display the numbers of genes which were differentially expressed and shared (common) among the infected organs for each route of infection. There were 31 and 19 common genes from i.p. and i.n. infected animals, respectively. These common genes are listed and detailed in Tables 3 and 4. Interestingly, there were four common genes differentially expressed in all six organ infection models. These included BPSL3050 (*trpE*, anthranilate synthase component 1), BPSL2902 (putative phosphoglycerate mutase), BPSL2082 (conserved hypothetical protein), and BPSL0317 (conserved hypothetical protein). All four genes were highly up-regulated in all organs.

(ii) Common genes and types of infected organs. There were 292, 27, and 24 genes differentially expressed and shared (common) between i.p. and i.n. infected animals from the liver, lung, and spleen, respectively (Fig. 3). The Student *t* test was used to evaluate whether the relative transcriptional levels (mean $\log_2$ ratio) of the common genes were significantly different. The analysis revealed that the transcriptional levels of genes differentially expressed and shared between the i.p. and i.n. infection models were not significantly different ($P > 0.05$). We noted that the proportion of the shared genes among i.p. and i.n. infections was significantly low as seen in the lungs and spleens. This would suggest different gene expression profiles between i.p. and i.n. infections especially in the lungs and spleens. However, the common genes found between two different routes of the infection would demonstrate a similar status of bacterial response during the infection. A list of the common genes between i.p. and i.n. in each group of the organ types is found in Tables 7 to 9 posted at ftp://136.159.173.80/.

Bacterial growth and adaptation to the host environment during infection. (i) Determination of bacterial growth status during infection. Microarray data revealed significant differences in gene expression between *B. pseudomallei* grown in vivo and that grown in vitro. One major difference was a reduced expression of genes known to be involved in bacterial

TABLE 3. List of 31 common genes of *B. pseudomallei* differentially expressed in all three organ infection models following i.p. inoculation

Gene	Annotation	Expression level for organ and preparation no.											
		Liver				Lung				Spleen			
		1		2		1		2		1		2	
		Mean[a]	SD	Mean[a]	SD	Mean[a]	SD	Mean[a]	SD	Mean[a]	SD	Mean[a]	SD
BPSL0004	*hupA*, DNA-binding protein HU-alpha	−4.22	0.46	−5.86	0.66	−6.68	1.57	−4.15	0.90	−5.68	1.70	−5.04	0.67
BPSL0060	AraC family transcriptional regulator	2.49	0.65	3.36	0.36	2.62	0.48	1.07	0.24	2.13	0.24	2.81	0.84
BPSL0117	LysR family transcription regulatory protein	3.84	1.05	5.50	0.77	2.89	0.89	3.17	1.06	4.85	2.22	4.23	0.92
BPSL0317	Conserved hypothetical protein	3.80	0.36	3.87	0.61	4.42	0.52	2.53	0.41	3.22	1.54	4.66	0.74
BPSL0379	Putative short-chain dehydrogenase	−4.11	1.03	−3.93	0.54	−3.66	0.53	−2.91	0.96	−2.87	0.49	−2.18	0.82
BPSL0430	Putative thioesterase	5.14	0.54	4.41	0.33	3.08	0.53	2.25	1.11	1.93	0.38	3.78	0.48
BPSL0522	Putative membrane protein	−8.78	1.06	−5.96	0.59	−8.49	1.30	−4.12	0.45	−6.34	2.93	−5.52	0.87
BPSL0635	Conserved hypothetical protein	−5.19	1.05	−4.97	0.81	−3.11	0.83	−5.49	1.47	−3.25	0.34	−2.69	0.98
BPSL1058	Putative transposase	−9.40	1.03	−7.52	0.37	−6.93	0.64	−8.24	2.30	−7.34	0.42	−6.02	0.56
BPSL1119	Putative lipopolysaccharide biosynthesis-related protein	4.62	0.46	5.37	0.23	3.45	0.76	3.04	1.39	4.96	0.93	4.70	1.27
BPSL1356	*ftsH*, cell division protein	−3.11	0.34	−3.40	0.37	−2.85	0.20	−3.09	0.63	−2.73	0.12	−4.07	0.76
BPSL1392	Hypothetical protein	3.63	1.43	5.59	0.62	3.05	0.57	1.88	0.20	2.78	1.10	5.40	1.74
BPSL1592A	Conserved hypothetical protein	−5.57	0.25	−4.79	0.29	−4.43	0.75	−4.77	0.99	−4.00	0.45	−3.58	0.37
BPSL1836	*cysA*, sulfate transport ATP-binding protein	4.20	0.49	4.58	0.45	3.56	0.08	1.78	0.38	3.45	0.81	4.65	0.52
BPSL2040	Hypothetical protein	4.32	0.78	5.31	0.96	4.41	0.77	2.91	0.75	3.60	0.92	5.82	0.90
BPSL2082	Conserved hypothetical protein	4.34	1.72	6.26	0.95	4.72	0.87	2.40	0.48	5.18	0.73	5.74	1.57
BPSL2219	Putative phosphoserine aminotransferase	−5.40	1.15	−3.40	0.28	−3.28	0.70	−3.76	0.26	−3.89	1.30	−2.36	0.48
BPSL2557	*cspA*, cold shock-like protein	−6.15	2.79	−8.83	0.57	−7.20	1.88	−5.22	1.86	−5.62	1.12	−5.11	0.79
BPSL2881	Putative membrane protein	−6.99	0.26	−4.74	1.10	−4.39	1.15	−4.86	1.52	−3.44	0.83	−1.83	0.24
BPSL2902	Putative phosphoglycerate mutase	4.19	0.93	5.17	0.38	2.73	0.96	2.20	0.63	3.25	0.43	4.31	0.72
BPSL3027	*murD*, UDP-*N*-acetylmuramoylalanine–D-glutamate ligase	5.03	0.63	4.81	0.38	2.48	1.12	3.27	1.62	2.97	0.55	2.59	0.38
BPSL3050	*trpE*, anthranilate synthase component 1	3.94	1.93	5.42	0.33	2.72	0.81	2.24	1.02	2.49	0.70	3.55	1.26
BPSL3085	Conserved hypothetical protein	−3.46	0.29	−2.87	0.16	−2.56	0.60	−3.62	1.12	−2.60	0.67	−2.07	0.58
BPSL3253	Putative oxidoreductase	4.83	1.18	4.82	0.58	3.05	0.92	2.90	1.05	3.56	1.18	2.15	0.52
BPSS0515	Hypothetical protein	−6.63	0.6	−5.21	0.90	−5.35	2.04	−6.03	1.52	−4.40	1.62	−3.02	0.17
BPSS0965	Putative oxalate decarboxylase	3.81	0.48	5.93	0.20	3.47	0.21	2.25	1.04	3.93	0.15	3.96	1.35
BPSS1199	Hypothetical protein	−6.11	1.73	−7.50	0.63	−6.96	1.95	−4.64	2.01	−6.18	1.83	−4.96	0.1
BPSS1388	Putative membrane protein	5.56	1.53	7.86	1.05	5.40	1.33	2.34	0.65	4.59	0.44	5.14	1.36
BPSS1489	Putative exported protein	5.94	0.53	7.45	0.37	3.97	0.40	2.68	1.34	3.64	0.13	4.53	1.17
BPSS1933	Putative membrane protein	−6.43	0.58	−4.67	0.54	−4.05	0.64	−4.63	2.07	−4.51	0.38	−3.82	0.36
BPSS2229	Conserved hypothetical protein	2.90	1.08	3.45	0.27	2.40	1.04	2.22	0.43	2.02	0.44	3.25	1.11

[a] Mean value is mean $\log_2$ ratio (in vivo/in vitro) calculated from two replicates.

growth and multiplication. These included genes coding for ribosomal proteins (BPSL3206, BPSL2911, etc.) and a cell division protein (*ftsH*, BPSL1356). This was clearly seen in data obtained from most organ infection models except the i.n. lungs and i.n. spleens where the ribosomal protein and cell division protein genes were not differentially expressed. The overall gene expression profile for ribosomal protein genes is shown in Fig. 1 posted at ftp://136.159.173.80/. Interestingly, *rpsA* (BPSL2515, 30S ribosomal protein S1), a housekeeping gene, was highly up-regulated, especially in infected liver. In addition, we also found that an equal amount of total bacterial RNA purified from all tested organs contained less rRNA than that isolated from broth culture. This observation was confirmed by quantitative RT-PCR of the 16S and 23S rRNA genes from both sources of the total RNA samples. The results clearly showed a higher quantity of PCR products of those two target genes from the total RNA isolated from the broth culture relative to infected tissues (see Fig. 5 posted at ftp://136.159.173.80/). Thus, we used purified bacterial mRNA instead of total RNA for microarray analyses in our studies.

(ii) Biochemical pathways. Gene expression profiles revealed that a number of genes for various metabolic enzymes were differentially expressed between in vivo- and in vitro-grown *B. pseudomallei*. We used information available for *B. pseudomallei* biochemical pathways from GenomeNet at The Bioinformatics Centre, Kyoto University, Japan (http://www.genome.jp), together with genome annotation information (13) as a guide to interpret our microarray data. We observed that most genes coding for proteins involved in carbohydrate metabolism including several biochemical pathways such as glycolysis, citrate cycle (tricarboxylic acid [TCA] cycle), pentose phosphate pathway, etc., were not differentially expressed, except for a few genes which were highly up- or down-regulated. The highly up-regulated genes were those coding for proteins known or predicted to be involved in (i) an intermediate step of the glycolytic pathway (or known as the first substrate-level intermediate such as a phosphoglycerate mutase [BPSL2902]), (ii) inositol catabolism (BPSL1996 and BPSL1997), and (iii) glucosamine catabolism such as the *glmS3* gene (BPSS2009, glucosamine–fructose-6-phosphate aminotransferase). In contrast, the highly down-regulated genes were genes coding for proteins associated with the TCA cycle such as BPSL0373 (putative isocitrate dehydrogenase), BPSL2469 (*fumC*, fumarate hydratase), BPSL0780 (*sucD*, succinyl coenzyme A [CoA] ligase), BPSS1916 (*phbB*, acetoacetyl-CoA re-

TABLE 4. List of 19 common genes of *B. pseudomallei* differentially expressed in all three organ infection models following i.n. inoculation

Gene	Annotation	Expression level for organ and preparation no.											
		Liver				Lung				Spleen			
		1		2		1		2		1		2	
		Mean[a]	SD	Mean[a]	SD	Mean[a]	SD	Mean[a]	SD	Mean[a]	SD	Mean[a]	SD
BPSL0308	Putative exported protein	3.58	0.10	3.71	0.23	3.20	0.37	2.41	0.56	3.09	1.26	2.88	1.27
BPSL0317	Conserved hypothetical protein	3.37	0.64	3.95	0.43	2.56	0.51	4.51	0.57	3.16	1.54	3.38	1.29
BPSL0500	Putative chitobiase	2.70	0.65	3.52	0.56	3.01	0.95	2.04	0.76	2.76	1.11	2.70	1.12
BPSL0548	Hypothetical protein	4.43	0.38	4.46	1.23	2.44	0.86	3.98	1.17	3.49	0.35	3.43	0.50
BPSL0959	*cysD*, putative sulfate adenylyltransferase subunit 2	4.76	0.52	5.97	0.81	3.98	0.66	3.58	1.47	3.14	1.21	3.42	0.78
BPSL2082	Conserved hypothetical protein	4.29	0.38	5.32	0.69	5.79	0.64	4.64	1.27	3.19	0.92	3.12	1.55
BPSL2696	Putative kinase	5.30	0.47	6.78	0.66	5.15	0.62	6.62	2.33	4.57	1.51	4.80	1.62
BPSL2756	Putative exported protein	2.74	0.20	3.17	0.47	3.30	0.40	2.91	0.47	2.65	1.14	2.67	1.26
BPSL2786	Putative acetyltransferase protein	4.07	0.59	5.49	0.19	3.86	0.56	2.89	0.44	2.39	0.58	2.63	0.59
BPSL2859	Conserved hypothetical protein	2.78	0.38	3.76	0.59	2.13	0.49	4.16	1.08	2.90	0.93	3.07	0.66
BPSL2902	Putative phosphoglycerate mutase	3.73	0.75	4.73	0.27	2.61	0.64	3.12	1.17	4.88	2.06	5.04	1.65
BPSL3050	*trpE*, anthranilate synthase component 1	3.29	0.46	4.57	0.35	2.22	0.67	2.42	0.81	2.20	0.47	2.29	0.75
BPSS0163	*asnO* gene, asparagine synthetase (glutamine hydrolyzing)	4.40	0.36	4.89	0.78	2.43	0.23	2.84	0.96	2.50	0.72	2.45	0.76
BPSS0204	*tsr* gene, methyl-accepting chemotaxis protein I	3.53	0.86	4.73	0.27	3.47	0.82	2.74	1.06	3.65	1.29	3.79	0.84
BPSS0464	*potI* gene, putrescine transport system permease protein	4.69	0.51	5.21	1.09	3.58	1.32	3.41	1.10	5.19	0.91	4.58	0.66
BPSS0622	Enoyl-CoA hydratase/isomerase family	3.56	0.43	3.55	0.43	3.19	0.71	4.12	0.80	3.58	0.73	3.66	0.84
BPSS0834	Hypothetical protein	3.83	0.65	4.63	0.37	3.05	0.93	4.40	0.77	2.86	0.76	3.06	0.64
BPSS0909	OmpA family protein	3.79	0.43	5.06	0.73	4.94	0.42	6.02	1.40	2.47	1.12	2.65	0.81
BPSS0925	Short-chain dehydrogenase	3.03	0.28	3.70	0.26	4.25	0.83	4.75	1.13	3.36	1.25	3.67	1.18

[a] Mean value is mean $\log_2$ ratio (in vivo/in vitro) calculated from two replicates.

ductase), etc. These down-regulated genes were mostly found in the infected livers from both i.p. and i.n. infected animals.

Moreover, genes coding for proteins involved in catabolism and synthesis of particular amino acids were highly differentially expressed, while most genes were not differentially expressed. The highly up-regulated genes were genes BPSL3050 (*trpE*, anthranilate synthase component 1), BPSS0163 (*asnO*, asparagine synthase), BPSL2260 (putative tryptophanyl-tRNA synthase), and BPSS2009 (*glmS3*, glucosamine–fructose-6-phosphate aminotransferase), etc. The down-regulated genes were genes coding for proteins associated with serine catabolism/synthesis including BPSS0547 (*glyA*, serine hydroxymethyltransferase) and BPSL2219 (putative phosphoserine aminotransferase). These differentially expressed genes were mostly found in infected livers and i.n. infected lungs.

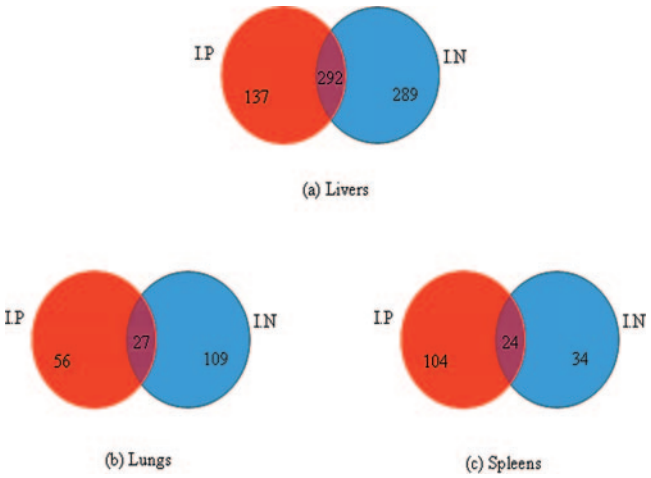

FIG. 3. Venn diagrams showing numbers of common genes differentially expressed and associated with infected organ types, livers (a), lungs (b), and spleens (c), for i.p. and i.n. routes of infection. Transcriptional levels of the common genes between i.p. and i.n. routes of each type of the organs were not significantly different.

In addition to the metabolic genes described above, we also observed that most genes coding for proteins commonly involved in energy metabolism such as ATP-synthase (BPSL3401, BPSS1953, etc.) and NADH-dehydrogenase enzymes (BPSL 1223, BPSL1224, etc.) were down-regulated. However, oxidative phosphorylation genes coding for enzymes involved in metabolism of alternative energy sources such as the genes *cyoA* (BPSS1897) and *cyoB* (BPSS1896), coding for ubiquinol oxidase; BPSS0555, coding for ferredoxin oxidoreductase; and BPSL2528 (*fdsG*), coding for NAD-dependent formate dehydrogenase, were highly induced. This provided evidence for the use of alternative pathways for energy during slower growth in infected organs. Figures 2 to 4 posted at ftp://136.159.173.80/ display an overview of metabolic genes and their expression profiles in all six organ infection models.

Expression profile of known virulence genes. We observed several groups of genes coding for proteins which have been well characterized and known to be involved in bacterial pathogenesis and virulence in *B. pseudomallei*. These included genes for capsular biosynthesis, type III secretion system (TTSS), and flagellar biosynthesis and secreted hydrolytic enzymes such as phospholipases and proteases. We found that a putative acetyltransferase gene (BPSL2786) involved in capsular biosynthesis was highly up-regulated in most organ infection models except in one out of two replicates of the i.p. infected lungs (Fig. 4).

FIG. 4. Gene expression profile in vivo versus in vitro for capsular biosynthesis genes. A particular gene coding for acetyltransferase enzyme activity (BPSL2786) was highly up-regulated, while most genes for the capsular biosynthesis were not differentially expressed. LPS, lipopolysaccharide.

In addition, at least two genes in TTSS such as BPSS1526 (putative invasion protein) and BPSS1530 (putative H-NS-like regulatory protein) were up-regulated in infected livers. Furthermore, BPSS1489, a possible additional gene in TTSS3 (25), was also highly up-regulated in most tested organs. We also observed that two genes involved in flagellar biosynthesis, including *fliD* (BPSL3320, flagellar hook-associated protein) and *flhC* (BPSL3310, flagellar regulon master regulator subunit FlhC), were highly up-regulated, while the *fliC* gene (BPSL3319, flagellin) was strongly down-regulated (Fig. 5). We also found that genes coding for phospholipase enzymes such as genes BPSS0067 (nonhemolytic phospholipase C) and BPSS1876 (putative phospholipase) were strongly up-regulated, especially in infected liver.

Virulence assessment of *B. pseudomallei* mutant strains. To validate the microarray data, at least 11 highly up-regulated genes from this study were characterized by insertional mutagenesis and the mutants were evaluated for virulence in the hamster model of acute melioidosis. The mutant strains ATL0378, ATL1876, ATL2025, ATL2515, ATL3050, ATL3320, ATS0067, ATS0464, ATS1388, ATS1489, and ATS1530 were made from the mutation in genes BPSL0378, BPSL1876, BPSL2025, BPSL2515, BPSL3050, BPSL3320, BPSS0067, BPSS0464, BPSS1388, BPSS1489, and BPSS1530, respectively. These genes have not previously been characterized in any study before and were chosen based on their various putative functions such as genes for bacterial growth and metabolism (i.e., BPSL2515, BPSL3050, and BPSS0464), regulatory systems (i.e., BPSL0378 and BPSS1530), and putative virulence molecules (i.e., BPSL1876, BPSL3320, and BPSS0067) and genes with unknown functions (i.e., BPSL2025, BPSS1388, and BPSS1489). Our data showed that only the mutants ATL2025 and ATS0067 had significant LD_{50} values higher than that of the parent strain *B. pseudomallei* DD503, which were determined to be 1.4×10^4 and 4.5×10^4 CFU, respectively. In addition, two complemented mutants, ATCPL2025 and ATCPS0067, were also evaluated for virulence in the hamster model. We found that both complemented mutants were able

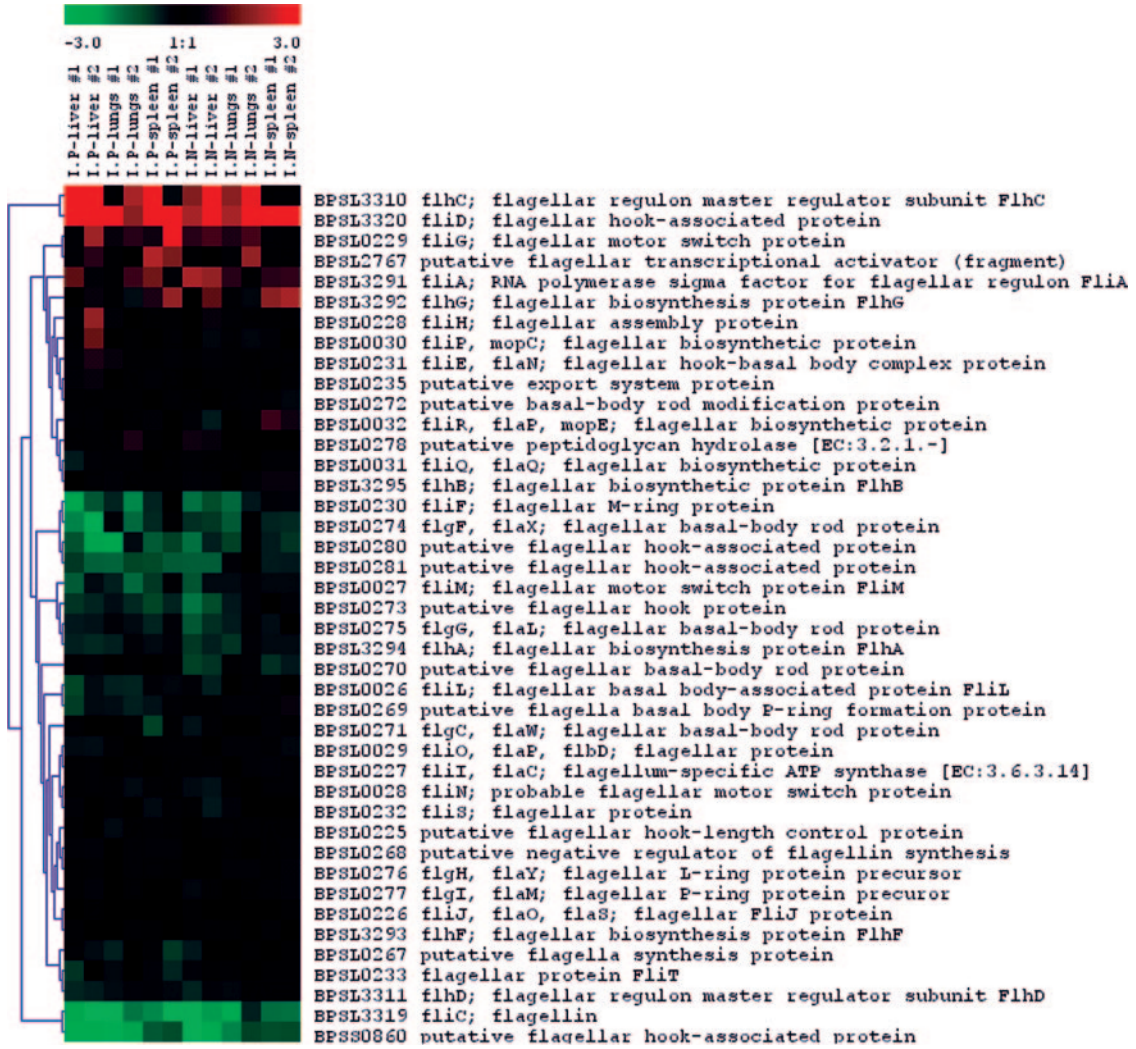

FIG. 5. Gene expression profile in vivo versus in vitro of flagellar biosynthesis genes. The *fliC* gene coding for flagellin was significantly down-regulated, while *fliD*, encoding a flagellar hook-associated protein, was highly induced. Most flagellar biosynthesis genes were not differentially expressed.

to restore the virulence in hamsters to levels equivalent to that of the wild-type strain. Details of the insertional mutants and their virulence assessment data are shown in Table 5.

DISCUSSION

The current studies detail the results from the analysis of gene expression in *B. pseudomallei* in an animal model of acute melioidosis using whole-genome microarrays and comparing different routes of infection. Recently, the relationship between routes of infection and virulence of *B. pseudomallei* has been investigated in BALB/c and C57BL/6 mouse models of systemic melioidosis (2). This study demonstrated that the virulence of *B. pseudomallei* is dependent upon the route of infection. LD_{50} values for animals infected with *B. pseudomallei* inoculated subcutaneously, intranasally, and orally were higher than those for animals inoculated intravenously or intraperitoneally. In our present studies, we used the hamster infection model of systemic acute melioidosis, as hamsters are exquisitely sensitive to *B. pseudomallei* and do not display individual susceptibility variation (10).

Our studies have conclusively demonstrated that *B. pseudomallei* genes are differentially expressed in vivo compared to in vitro growth. A number of genes were up- or down-regulated in infected organs, especially in the liver. Gene expression profiles and additional evidence demonstrated that bacterial growth in infected organs was slower than growth at mid-exponential phase in LB medium. This was demonstrated by reduced expression of numerous housekeeping genes coding for bacterial growth and multiplication proteins including genes for ribosomal proteins and cell division proteins. Interestingly, the total bacterial RNA from infected tissues contained lower amounts of rRNA than did that from organisms grown in LB. Thus, it could be suggested that the lower growth rate of *B. pseudomallei* in infected organs characterizes acute melioidosis in the hamster model. Further, the identification of the differentially expressed genes in these organs provides an understanding of bacterial response to the host environment

TABLE 5. Virulence assessments of *B. pseudomallei* mutants in the hamster model of acute melioidosis

Strain	Description/gene for mutation	LD_{50} (CFU)
DD503	Parent strain	<10
ATL0378	ΔBPSL0378 (MarR family regulatory protein)	<10
ATL1876	ΔBPSL1876 (putative phospholipase)	<10
ATL2025	ΔBPSL2025 (putative two-component regulatory system)	1.4×10^4
ATL2515	ΔBPSL2515 (*rpsA*; 30S ribosomal protein S1)	<10
ATL3050	ΔBPSL3050 (*trpE*; anthranilate synthase component 1)	<10
ATL3320	ΔBPSL3320 (*fliD*, flagellar hook-associated protein)	<10
ATS0067	ΔBPSS0067 (putative phospholipase C precursor)	4.5×10^4
ATS0464	ΔBPSS0464 (*potI*, putrescine transport system permease protein)	<10
ATS1388	ΔBPSS1388 (putative membrane protein)	<10
ATS1489	ΔBPSS1489 (putative exported protein)	<10
ATS1530	ΔBPSS1530 (*bprA*, putative H-NS-like regulatory protein)	<10
ATCPL2052	Complemented mutant of ATL2052	<10
ATCPS0067	Complemented mutant of ATS0067	<10

during the infection. A similar observation was found in a recent in vivo gene expression study of *B. mallei*, a closely related organism, using a mouse model of infection which demonstrated that a number of housekeeping genes and metabolic genes responsible for bacterial growth and multiplication were relatively reduced in expression (17).

Four genes were commonly found to be highly induced in vivo. These included gene *trpE* (anthranilate synthase component 1), a gene for a putative phosphoglycerate mutase, and two genes coding for conserved hypothetical proteins. The *trpE* gene codes for an enzyme anthranilate synthase known to be involved in tryptophan amino acid biosynthesis. It has been reported that mutagenesis of *trpE* and *aroA*, an essential gene in *Bordetella bronchiseptica*, produces an aromatic amino acid auxotrophic mutant, and this mutant has reduced abilities to invade and survive within the macrophage cells in vitro and in vivo. This mutant was also tested for its ability to serve as a potential live-attenuated vaccine against this pathogen (22). Another up-regulated gene, a putative phosphoglycerate mutase, is known to be involved in the isomerization of the first substrate-level intermediate, 3-phosphoglycerate, to produce 2-phosphoglycerate for ATP. This would suggest that the organism is able to access this high-energy molecule during infection. Functional information for *trpE*, BPSL2902, and the two conserved hypothetical protein genes in *B. pseudomallei* is presently unavailable. In addition, insertion mutagenesis of the *trpE* gene in *B. pseudomallei* did not reduce virulence in the hamster model of acute melioidosis.

Our studies have demonstrated that *B. pseudomallei* uses novel pathways to generate and maintain cellular energy in vivo. The down-regulation of genes coding for enzymes known to be involved in the glycolytic pathway and the TCA cycle could contribute to the lower growth rate in vivo. We have demonstrated that genes coding for enzymes involved in the catabolism of D-glucosamine, an amino sugar, and inositol are highly up-regulated. Both of these substrates could serve as alternative carbon sources for carbohydrate metabolism. In addition, the induced expression of specific amino acid catabolism and biosynthesis genes such as *asnO* (asparagine synthase) and BPSL2260 (putative tryptophanyl-tRNA synthase) suggests that the organism uses novel metabolic pathways for amino acid metabolism. In addition to the alternative pathways utilized for carbohydrate and amino acid metabolism during in vivo growth, genes coding for enzymes known or predicted to be involved in alternative energy metabolism such as ubiquinol oxidases were also induced. Further, genes coding for enzymes required for primary energy metabolism such as ATP-synthase and NADH-dehydrogenase were down-regulated. We made a similar observation for bacteria grown under low-iron conditions (33). In low-iron conditions which are postulated to imitate the host environment, siderophore biosynthesis genes including a hydroxamate siderophore and pyochelin as well as heme-hemin receptor transport protein genes are highly induced (33). In the present studies, the pyochelin biosynthesis gene (BPSS0588) was induced in infected livers (see Table 7 posted at ftp://136.159.173.80/). Multiple in vitro studies designed to mimic the host environment have identified the expression of genes necessary for bacterial growth and survival under these conditions. These in vitro studies have involved an examination of growth under oxidative stress and the identification of the expression of the *dpsA* gene as necessary for survival (21) and stress due to the presence of reactive nitrogen intermediates and the identification of the expression of the *ahpC-katG* genes as important for survival (20). In addition, macrophage killing assays have been used in several studies to mimic the environment of host defense mechanisms, and genes responsible for the bacterial protective mechanisms have been identified. In particular, expression of the type III secretion *bsa* genes has been shown to be involved in the induction of the caspase-1-dependent macrophage death (32) and shown to play an essential role in modulating the intracellular behavior of *B. pseudomallei* (31). Interestingly, these well-characterized genes were not found in any organ infection models in our present studies. This is likely due to the equal expression of these under in vivo and in vitro conditions. This same observation was noted with other genes known to be involved in virulence such as genes for capsular biosynthesis, other genes in the type III secretion system, and flagellar biosynthesis genes. The products of these genes have been demonstrated to be virulence determinants in various animal models. It is likely that the transcriptional levels of these genes are equal during in vivo and in vitro growth, as it is well known that capsule, flagellum, and other virulence determinants are constitutively produced in vitro.

Flagella have been shown to be a virulence determinant in the BALB/c mouse model; mutation in the *fliC* gene caused

virulence attenuation during intranasal and intraperitoneal infection in this animal model (7). *fliC* mutants remain highly virulent in the Syrian hamster and diabetic rat models (9). In the current studies, the *fliC* gene was strongly down-regulated, while *fliD*, a gene coding for a flagellar hook-associated protein, was highly induced (Fig. 5). An insertion mutation in the *fliD* gene did not lead to attenuation in the hamster infection model. These results confirm our earlier results indicating that flagella do not play a role in virulence in the hamster model of acute melioidosis. This would appear to be a deficiency of the hamster model, as the important role of flagella in different animal models of melioidosis is generally accepted, and a recent study has demonstrated the potential of using plasmid-encoded flagellin as a melioidosis vaccine (5).

Mutagenesis of a total of 11 up-regulated genes allowed us to identify two genes which were involved in virulence in the hamster model of acute melioidosis. These genes were BPSL2025 (putative two-component regulatory system) and BPSS0067 (putative phospholipase C precursor). A different two-component regulatory system known as *irlRS* has been characterized previously in *B. pseudomallei*, and its mutant was deficient in the ability to invade a human type II pneumocyte cell line, but it is not a virulence determinant in the infant diabetic rat and Syrian hamster models of acute *B. pseudomallei* infection (14). In addition, a different phospholipase C gene encoding a phosphatidylcholine-hydrolyzing phospholipase C (PC-PLC) has also been characterized previously in *B. pseudomallei*, and its product was recognized by human immunoglobulin M antibodies (18). However, there has been no report of this gene's involvement in bacterial virulence. Since our studies have shown a potential role of a putative two-component regulatory system (BPSL2025) and a putative phospholipase C (BPSS0067), a full understanding of these two genes in *B. pseudomallei* pathogenesis warrants further investigation. Our studies demonstrate the value of using gene expression profiles during bacterial infection in vivo combined with mutagenesis to identify potential virulence genes in *B. pseudomallei*.

In summary, our studies have identified differentially expressed genes which include potential virulence genes, and they have also provided a better understanding of bacterial metabolism in response to the host environment during acute melioidosis. The observation relative to the induction of specific genes for alternative biochemical pathways and a number of unknown genes most certainly warrants further experimentation.

ACKNOWLEDGMENTS

This work was funded by the Canadian Institutes of Health research grant MOP-36343 to D.E.W., a Canada Research Chair in Microbiology. The printing of the *B. pseudomallei* whole-genome microarray slides was supported by a Los Alamos Research and Development grant to J.D.

We thank Mayi Arcellana-Panlillo and Xiuling Wang at the Southern Alberta Microarray Facilities, University of Calgary, for technical assistance, and we also thank Paige Pardington and Robert Cary at Los Alamos National Laboratory for printing the *B. pseudomallei* whole-genome microarray slides.

REFERENCES

1. **Allworth, A. M.** 2005. Tsunami lung: a necrotising pneumonia in survivors of the Asian tsunami. Med. J. Aust. **182:**364.
2. **Barnes, J. L., and N. Ketheesan.** 2005. Route of infection in melioidosis. Emerg. Infect. Dis. **11:**638–639.
3. **Brett, P. J., D. DeShazer, and D. E. Woods.** 1997. Characterization of *Burkholderia pseudomallei* and *Burkholderia pseudomallei*-like strains. Epidemiol. Infect. **118:**137–148.
4. **Chaowagul, W., N. J. White, D. A. Dance, Y. Wattanagoon, P. Naigowit, T. M. Davis, S. Looareesuwan, and N. Pitakwatchara.** 1989. Melioidosis, a major cause of community-acquired septicemia in northeastern Thailand. J. Infect. Dis. **159:**890–899.
5. **Chen, Y. S., Y. S. Hsiao, H. H. Lin, C. M. Yen, S. C. Chen, and Y. L. Chen.** 2006. Immunogenicity and anti-*Burkholderia pseudomallei* activity in Balb/c mice immunized with plasmid DNA encoding flagellin. Vaccine **24:**750–758.
6. **Cheng, A. C., J. N. Hanna, R. Norton, S. L. Hills, J. Davis, V. L. Krause, G. Dowse, T. J. Inglis, and B. J. Currie.** 2003. Melioidosis in Northern Australia, 2001-02. Commun. Dis. Intell. **27:**272–277.
7. **Chua, K. L., Y. Y. Chan, and Y. H. Gan.** 2003. Flagella are virulence determinants of *Burkholderia pseudomallei*. Infect. Immun. **71:**1622–1629.
8. **Dance, D. A.** 2000. Melioidosis as an emerging global problem. Acta Trop. **74:**115–119.
9. **DeShazer, D., P. J. Brett, R. Carlyon, and D. E. Woods.** 1997. Mutagenesis of *Burkholderia pseudomallei* with Tn*5*-OT182: isolation of motility mutants and molecular characterization of the flagellin structural gene. J. Bacteriol. **179:**2116–2125.
10. **DeShazer, D., and D. E. Woods.** 1999. Animal models of melioidosis, p. 199–203. *In* O. Zak and M. Sande (ed.), Handbook of animal models of infection. Academic Press, London, United Kingdom.
11. **DeShazer, D., and D. E. Woods.** 1999. Pathogenesis of melioidosis: use of Tn*5*-OT182 to study the molecular basis of *Burkholderia pseudomallei* virulence. J. Infect. Dis. Antimicrob. Agents **16:**91–96.
12. **Gan, Y. H., K. L. Chua, H. H. Chua, B. Liu, C. S. Hii, H. L. Chong, and P. Tan.** 2002. Characterization of *Burkholderia pseudomallei* infection and identification of novel virulence factors using a *Caenorhabditis elegans* host system. Mol. Microbiol. **44:**1185–1197.
13. **Holden, M. T., R. W. Titball, S. J. Peacock, A. M. Cerdeno-Tarraga, T. Atkins, L. C. Crossman, T. Pitt, C. Churcher, K. Mungall, S. D. Bentley, M. Sebaihia, N. R. Thomson, N. Bason, I. R. Beacham, K. Brooks, K. A. Brown, N. F. Brown, G. L. Challis, I. Cherevach, T. Chillingworth, A. Cronin, B. Crossett, P. Davis., D. DeShazer, T. Feltwell, A. Fraser, Z. Hance, H. Hauser, S. Holroyd, K. Jagels, K. E. Keith, M. Maddison, S. Moule, C. Price, M. A. Quail, E. Rabbinowitsch, K. Rutherford, M. Sanders, M. Simmonds, S. Songsivilai, K. Stevens, S. Tumapa, M. Vesaratchavest, S. Whitehead, C. Yeats, B. G. Barrell, P. C. Oyston, and J. Parkhill, J.** 2004. Genomic plasticity of the causative agent of melioidosis, *Burkholderia pseudomallei*. Proc. Natl. Acad. Sci. USA **101:**14240–14245.
14. **Jones, A. L., D. DeShazer, and D. E. Woods.** 1997. Identification and characterization of a two-component regulatory system involved in invasion of eukaryotic cells and heavy-metal resistance in *Burkholderia pseudomallei*. Infect. Immun. **65:**4972–4977.
15. **Jones, A. L., T. J. Beveridge, and D. E. Woods.** 1996. Intracellular survival of *Burkholderia pseudomallei*. Infect. Immun. **64:**782–790.
16. **Kespichayawattana, W., P. Intachote, P. Utaisincharoen, and S. Sirisinha.** 2004. Virulent *Burkholderia pseudomallei* is more efficient than avirulent *Burkholderia thailandensis* in invasion of and adherence to cultured human epithelial cells. Microb. Pathog. **36:**287–292.
17. **Kim, H. S., M. A. Schell, Y. Yu, R. L. Ulrich, S. H. Sarria, W. C. Nierman, and D. DeShazer.** 2005. Bacterial genome adaptation to niches: divergence of the potential virulence genes in three *Burkholderia* species of different survival strategies. BMC Genomics **6:**174.
18. **Korbsrisate, S., N. Suwanasai, A. Leelaporn, T. Ezaki, Y. Kawamura, and S. Sarasombath.** 1999. Cloning and characterization of a nonhemolytic phospholipase C gene from *Burkholderia pseudomallei*. J. Clin. Microbiol. **37:**3742–3745.
19. **Leaky, A. K., G. C. Ulett, and R. G. Hirst.** 1998. BALB/c and C57Bl/6 mice infected with virulent *Burkholderia pseudomallei* provide contrasting animal models for the acute and chronic forms of human melioidosis. Microb. Pathog. **24:**269–275.
20. **Loprasert, S., R. Sallabhan, W. Whangsuk, and S. Mongkolsuk.** 2003. Compensatory increase in *ahpC* gene expression and its role in protecting *Burkholderia pseudomallei* against reactive nitrogen intermediates. Arch. Microbiol. **180:**498–502.
21. **Loprasert, S., W. Whangsuk, R. Sallabhan, and S. Mongkolsuk.** 2004. DpsA protects the human pathogen *Burkholderia pseudomallei* against organic hydroperoxide. Arch. Microbiol. **182:**96–101.
22. **McArthur, J. D., N. P. West, J. N. Cole, H. Jungnitz, C. A. Guzman, J. Chin, P. R. Lehrbach, S. P. Djordjevic, and M. J. Walker.** 2003. An aromatic amino acid auxotrophic mutant of *Bordetella bronchiseptica* is attenuated and immunogenic in a mouse model of infection. FEMS Microbiol. Lett. **211:**7–16.
23. **Miller, W. R., L. Pannell, L. Cravitz, W. A. Tanner, and T. Rosebury.** 1948. Studies on certain biological characteristics of *Malleomyces mallei* and *Malleomyces pseudomallei*. II. Virulence and infectivity for animals. J. Bacteriol. **55:**127–135.
24. **Moore, R. A., D. DeShazer, S. Reckseidler, A. Weissmann, and D. E. Woods.**

1999. Efflux-mediated aminoglycoside and macrolide resistance in *Burkholderia pseudomallei*. Antimicrob. Agents Chemother. **43:**465–470.
25. **Moore, R. A., S. Reckseidler-Zenteno, H. Kim, W. C. Nierman, Y. Yu, A. Tuanyok, J. Warawa, D. DeShazer, and D. E. Woods.** 2004. The contribution of gene loss to the pathogenic evolution of *Burkholderia pseudomallei* and *Burkholderia mallei*. Infect. Immun. **72:**4172–4187.
26. **Ngauy, V., Y. Lemeshev, L. Sadkowski, and G. Crawford.** 2005. Cutaneous melioidosis in a man who was taken as a prisoner of war by the Japanese during World War II. J. Clin. Microbiol. **43:**970–972.
27. **O'Quinn, A. L., E. M. Wiegand, and J. A. Jeddeloh.** 2001. *Burkholderia pseudomallei* kills the nematode *Caenorhabditis elegans* using an endotoxin-mediated paralysis. Cell. Microbiol. **3:**381–393.
28. **Reed, L. J., and H. Muench.** 1938. A simple method of estimating fifty per cent endpoints. Am. J. Hyg. **27:**493–497.
29. **Rolim, D. B.** 2005. Melioidosis, northeastern Brazil. Emerg. Infect. Dis. **11:**1458–1460.
30. **Simon, R., U. Priefer, and A. Puhler.** 1983. A broad host range mobilization system for *in vivo* genetic engineering: transposon mutagenesis in gram negative bacteria. Bio/Technology **1:**784–791.
31. **Stevens, M. P., M. W. Wood, L. A. Taylor, P. Monaghan, P. Hawes, P. W. Jones, T. S. Wallis, and E. E. Galyov.** 2002. An Inv/Mxi-Spa-like type III protein secretion system in *Burkholderia pseudomallei* modulates intracellular behaviour of the pathogen. Mol. Microbiol. **46:**649–659.
32. **Sun, G. W., J. Lu, S. Pervaiz, W. P. Cao, and Y. H. Gan.** 2005. Caspase-1 dependent macrophage death induced by *Burkholderia pseudomallei*. Cell. Microbiol. **7:**1447–1458.
33. **Tuanyok, A., H. S. Kim, W. C. Nierman, Y. Yu, J. Dunbar, R. A. Moore, P. Baker, M. Tom, J. M. L. Ling, and D. E. Woods.** 2005. Genome-wide expression analysis of iron regulation in *Burkholderia pseudomallei* and *Burkholderia mallei* using DNA microarray. FEMS Microbiol. Lett. **252:**327–335.
34. **Warawa, J., and D. E. Woods.** 2005. Type III secretion system cluster 3 is required for maximal virulence of *Burkholderia pseudomallei* in a hamster infection model. FEMS Microbiol. Lett. **242:**101–108.
35. **West, S. E., H. P. Schweizer, C. Dall, A. K. Sample, and L. J. Runyen-Janecky.** 1994. Construction of improved *Escherichia-Pseudomonas* shuttle vectors derived from pUC18/19 and sequence of the region required for their replication in *Pseudomonas aeruginosa*. Gene **148:**81–86.
36. **White, N. J.** 2003. Melioidosis. Lancet **361:**1715–1722.
37. **Whitmore, A., and C. S. Krishnaswami.** 1912. An account of glander-like disease occurring in Rangoon. J. Hyg. **13:**1–34.
38. **Woods, D. E.** 2002. The use of animal infection models to study the pathogenesis of melioidosis and glanders. Trends Microbiol. **10:**483–484.

Editor: J. T. Barbieri